PAPER

# Interference Suppression Method between Primary Broadcasting and Secondary Systems Using Load Modulation

**Takuma ITO**[†a)], ***Student Member***, **Naoki HONMA**[†], ***Member***, **Keisuke TERASAKI**[†], ***Student Member***, **Kentaro NISHIMORI**[††], ***Senior Member***, ***and*** **Yoshitaka TSUNEKAWA**[†], ***Member***

**SUMMARY** Controlling interference from the secondary system (SS) to the receiver of the primary system (PS) is an important issue when the SS uses the same frequency band as the television broadcast system. The reason includes that the SS is unaware of the interference imposed on the primary receiver (PS-Rx), which does not have a transmitter. In this paper, we propose an interference control method between PS-Rx and SS, where a load modulation scheme is introduced to the PS-Rx. In this method, the signal from the PS transmitting station is scattered by switching its load impedance. The SS observes the scattered channel and calculates the interference suppression weights for transmitting, and controls interference by transmit beamforming. A simulation shows that the Signal-to-Interference Ratio (SIR) with interference control is improved by up to 41.5 dB compared to that without interference control at short distances; the results confirm that the proposed method is effective in controlling interference between PS-Rx and SS. Furthermore, we evaluate the Signal-to-Noise Ratio (SNR) and channel capacity at SS.

***key words:*** *load modulation, frequency sharing, interference control, channel capacity*

## 1. Introduction

The demand for frequency resources have been increasing because various wireless communication systems have been developed and released. However, the frequency band cannot be assigned arbitrary since the frequency resources are limited. Therefore, frequency sharing technologies among the multiple systems are required. However, co-channel interference between existing primary system (PS) and newly installed secondary system (SS) becomes one of important issues to be resolved when the same frequency band is used among them.

The frequency sharing technique using beam-forming (BF) at the SS base station (SS-BS) has been proposed [1]. The SS-BS suppresses the interference to the PS terminal by directing null directivity toward PS terminal. However, this technique cannot be applied to the situation where PS terminals do not have transmitters, such as TV receiver, since SS-BS cannot know the interference channel between SS-BS and PS receiver (PS-Rx). Further, cognitive radio technologies that improve the utilization of the frequency resources by observing the environment of other radio systems have been proposed [2]–[4]. Particularly, in [4], it is shown that the influence of interference from PS transmitting station (PS-Tx) to SS user equipment is evaluated when the SS is overlaid on the PS, i.e. TV system, and an algorithm for canceling the interference signal at SS user equipment is proposed. However, they have been only evaluated the performance of SS, and the effect of the interference suppression from SS-BS to TV receiver has not been investigated.

The target of this study is confirming an intersystem interference suppression method to realize frequency sharing between SS and PS, where PS terminals do not emit a radio wave, such as TV receiver. In this paper, we introduce a load modulation technique to PS-Rx in order to let SS-BS get the interference channel between PS-Rx and SS-BS. A load modulation is a technique that the terminal scatters and modulates the signal by switching the load impedance connected to the antenna [5]. This will enable PS-Rx to send the information to SS-BS without a transmitter by scattering the signal from PS-Tx. At the SS-BS, estimates the scattered channel and calculates the interference suppression weights for transmitting, and controls interference by BF [6].

Note that the term, 'load modulation', is used to explain varying the load impedance at the PS-Rx antenna, but the aim of this scheme is not for signal transmission to PS but for channel estimation at other system. Actually, the TV broadcast signal is already modulated signal, and varying impedance yields doubly modulated signal. Nevertheless, this scheme is physically identical to the existing load modulation technique, and the term, 'load modulation', is used in the following discussion.

## 2. Interference Control Method Using Load Modulation

Figure 1(a) shows the mechanism of load modulation. In this study, we use the bi-static structure, where the transmitting and receiving antennas at the reader are placed separately. The tag modulates and reflects the incident signal by switching the load impedance, $Z$, connected to the antenna at the terminal side [5]. The tag can send data without a transmitter using a carrier wave from the signal of reader-Tx side. At the reader-Rx, the modulated signal is decoded by observing its amplitude and phase, and can get information of the tag side. Also, the direct wave from reader-Tx reaches the reader-Rx. In this study, the load modulation

Manuscript received September 8, 2014.
Manuscript revised December 18, 2014.

[†]The authors are with the Graduate School of Engineering, Iwate University, Morioka-shi, 020-8551 Japan.
[††]The author is with the Graduate School of Science and Technology, Niigata University, Niigata-shi, 950-2181 Japan.
a) E-mail: t2313001@iwate-u.ac.jp

DOI: 10.1587/transcom.E98.B.861

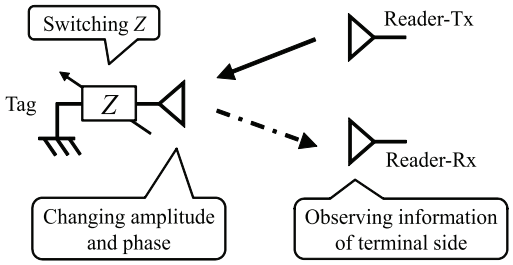


(a) The mechanism of load modulation (bi-static).

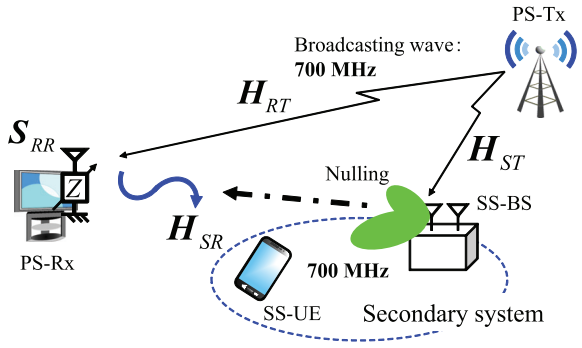


(b) Load modulation at the PS-Rx side and the structure of interference control.

**Fig. 1** Proposed system model.

scheme is utilized to estimate the channel, which is used for suppressing the interference from SS-BS to PS-Rx. Figure 1(b) shows load modulation at the PS-Rx side and the structure of interference suppression. This model assumes SS is overlaid on existing PS. SS has a base station (SS-BS) and user equipment (SS-UE), and each of them has multiple antennas. In PS, a receiver (PS-Rx) receives the signal from transmitting station (PS-Tx), and the number of the PS-Rx is set to one for simplicity since the transmitting power at SS-BS is assumed to be sufficiently small and the number of the PS-Rx can be one or less in the range where the signal reaches from SS. In this study, we assume that PS is a television broadcast system. The number of antennas of PS-Tx, PS-Rx and SS-BS are $M_{TT}$, $M_{RR}$, and $M_{SB}$, respectively, and $M_{TT} = M_{RR} = 1$. $Z$ is connected to PS-Rx antenna, and PS-Rx is able to reflect the broadcasting waves by switching $Z$. This allows SS-BS to receive the interference channel information.

Here, in this model, T, R, and S represent transmitting (PS-Tx antenna), terminal (PS-Rx antenna), and receiving (SS-BS antennas) ports, respectively. Figure 2 shows the antenna system model that includes not only PS-Tx and SS-BS antennas, but also antenna at the PS-Rx. A PS-Rx antenna is terminated by a tunable reactance, $Z$. The term $\boldsymbol{S}_S$ is the $S$-parameter matrix, and includes the $S$-parameter and channel matrix of both PS-Tx and SS-BS antennas. $a_T$ is the transmitted signal from T port, $\boldsymbol{a}_S = [a_{S_1}, \ldots, a_{S_{MSB}}]^T$ is the signals from S port, $a_R$ is the signal from R port, $b_T$ is the signal to T port, $\boldsymbol{b}_S = [b_{S_1}, \ldots, b_{S_{MSB}}]^T$ is the signals to S

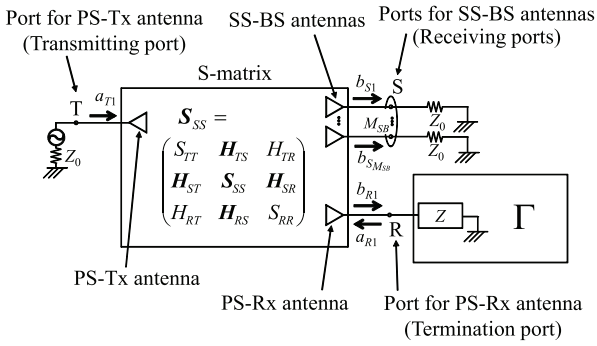


**Fig. 2** Equivalent circuit model of proposed system.

port, and $b_R$ is the signal to R port, where $[\cdot]^T$ is the matrix transposition. The relationship between $b_T$, $\boldsymbol{b}_S$ and $b_R$ can be expressed as [7]–[9],

$$\begin{pmatrix} b_T \\ \boldsymbol{b}_S \\ b_R \end{pmatrix} = \begin{pmatrix} S_{TT} & \boldsymbol{H}_{TS} & H_{TR} \\ \boldsymbol{H}_{ST} & \boldsymbol{S}_{SS} & \boldsymbol{H}_{SR} \\ H_{RT} & \boldsymbol{H}_{RS} & S_{RR} \end{pmatrix} \begin{pmatrix} a_T \\ \boldsymbol{a}_S \\ a_R \end{pmatrix} \tag{1}$$

$$a_R = \Gamma b_R, \tag{2}$$

where $S_{TT}$ and $\boldsymbol{S}_{SS}$ are the scattering matrices for the transmitting and SS-BS antennas, respectively. The term $S_{RR}$ ($\in \mathbb{C}^{M_{RR} \times M_{RR}}$) is the scattering coefficient of the PS-Rx antenna, and $\boldsymbol{H}_{RS}$ ($\in \mathbb{C}^{M_{RR} \times M_{SB}}$) represents the channel between SS-BS and PS-Rx antennas. Terms $\boldsymbol{H}_{ST}$ ($\in \mathbb{C}^{M_{SB} \times M_{TT}}$) and $H_{RT}$ ($\in \mathbb{C}^{M_{RR} \times M_{TT}}$) denote the channels from PS-Tx antenna to SS-BS antennas and PS-Rx antenna, respectively. Since the matrix is symmetric, $\boldsymbol{H}_{TS} = \boldsymbol{H}_{ST}^T$ ($\in \mathbb{C}^{M_{TT} \times M_{SB}}$) and $\boldsymbol{H}_{SR} = \boldsymbol{H}_{RS}^T$ ($\in \mathbb{C}^{M_{SB} \times M_{RR}}$). From the relationship shown in (1) and (2), the observed signal at S port is described as,

$$\begin{aligned} \boldsymbol{b}_S &= \{\boldsymbol{H}_{ST} + \boldsymbol{H}_{SR}\Gamma(1 - S_{RR}\Gamma)^{-1}H_{RT}\}a_T \\ &= \boldsymbol{H}'_{ST}a_T, \end{aligned} \tag{3}$$

where $\boldsymbol{H}'_{ST}$ ($\in \mathbb{C}^{M_{SB} \times M_{TT}}$) is the observed propagation channel at SS-BS which consists of both a direct path and path via PS-Rx. $\Gamma$ denotes the reflection coefficient of $Z$, and is expressed as,

$$\Gamma = \frac{Z - Z_0}{Z + Z_0}. \tag{4}$$

First, the channel, $\boldsymbol{H}_{SR}$, with ideal load ($Z_0$) is calculated in the ring model, which is explained in Sect. 3, and then, the interaction between $S_{RR}$ and load impedance and its effect of the load on the channel is calculated by (3). $Z_0$ is the reference impedance and the value is 50 Ω, and the state of $Z$ is open ($\infty$) or load (50 Ω). Here, PS-Rx switches $Z$ during PS-Rx does not receive signals, i.e. TV is not used. But this scheme is applicable when we have sufficiently stable environment, where the channel varies little. Nevertheless, it was recently shown that the channel in the indoor environment is fairly stable. In [10], the Doppler characteristics for wireless LAN in an indoor environment were experimentally evaluated, and it showed the temporal channel variance is much smaller than it has been believed as in the IEEE

802.11n standardization. Therefore, this paper assumes the channel is sufficiently stable for this reason and simplicity of the discussion. Otherwise, PS-Rx can receive and reflect the PS-Tx signal simultaneously if a part of the received power is used for the backscattering. This can be realized by inserting variable impedance element to the feed circuit, for example, the varactor diode is attached on the transmission line between antenna and receiver at PS-Rx [11]. However, the latter scheme is not dealt with in this paper because this needs further investigation and discussions. In the case of open, SS-BS observes the sum of the reflected wave from PS-Rx and direct wave from PS-Tx because PS-Rx reflects all broadcasting waves, and $\boldsymbol{H}'_{ST}$ can be transformed into,

$$\boldsymbol{H}'_{ST(open)} = \boldsymbol{H}_{ST} + \boldsymbol{H}_{SR}(1 - S_{RR})^{-1}H_{RT}. \quad (5)$$

On the other hand, when $Z$ is switched to load, only the direct wave from PS-Tx is observed at SS-BS because PS-Rx does not reflect the broadcasting wave, and (3) is transformed to,

$$\boldsymbol{H}'_{ST(load)} = \boldsymbol{H}_{ST}. \quad (6)$$

By (5) and (6), SS-BS can estimate $\boldsymbol{H}'_{SR}$, which is the channel from PS-Tx by way of PS-Rx. It can be expressed as,

$$\boldsymbol{H}'_{SR} = \boldsymbol{H}_{SR}(1 - S_{RR})^{-1}H_{RT}. \quad (7)$$

By singular value decomposition (SVD) of the transposed matrix of $\boldsymbol{H}'_{SR}$, we get,

$$\boldsymbol{H}'^{T}_{SR} = \boldsymbol{U}_{RS}[\boldsymbol{S}_{RS}, 0][\bar{\boldsymbol{V}}_{RS}, \tilde{\boldsymbol{V}}_{RS}]^{H}, \quad (8)$$

where $\tilde{\boldsymbol{V}}_{RS}$ is the null-space weight vectors from SS-BS. i.e., SS-BS can suppress interference by using $\tilde{\boldsymbol{V}}_{RS}$ as the transmitting weight. However, the channel received by SS-BS will contain noise, so we need to consider the effect of noise on BF accuracy. Although the signal from PS-Tx can be modulated, pilot signals for synchronization can be used, for example [12].

Note that both $\boldsymbol{H}_{SR}$ and $\boldsymbol{H}'_{SR}$ can be used for the weight calculation, but $\boldsymbol{H}'_{SR}$ is used instead of $\boldsymbol{H}_{SR}$ because information of $\boldsymbol{H}_{SR}$ is not available in an actual operation. Also, the proposed method is applicable to a case that PS-Tx and PS-Rx have multiple antennas. However, $M_{RR} < M_{SB}$ since the null directivity of SS-BS antenna is produced [13].

## 3. Simulation Setup

Table 1 shows the simulation conditions. $\lambda$ represents wavelength, and the amplitudes of transmitted signal and noise at SS-BS are in a Gaussian distribution. All antennas are dipoles. PS-Tx and PS-Rx have one antenna each while SS-BS has two; SS-BS antenna element spacing is 0.5 $\lambda$. In this study, the frequency lies in the 700 MHz band and the transmitted power of PS-Tx is set to 60 dBm since we assume a television broadcast system. The noise power in this paper is set to −100 dBm since we have considered that the simulation condition should be sufficiently feasible [14]. As the path-loss model, we use Okumura-Hata model for $H_{RT}$ and

**Table 1** Simulation condition.

| | |
|---|---|
| Antenna element | Dipole antenna |
| Number of antennas | PS-Tx: 1<br>PS-Rx: 1<br>SS-BS: 2 |
| SS-BS element spacing | 0.5 $\lambda$ |
| Frequency | 700 MHz |
| PS-Tx power | 60 dBm |
| Noise power at SS-BS | −100 dBm |
| Height | PS-Tx: 100 m<br>PS-Rx: 10 m<br>SS-BS: 10 m |
| Path-loss between PS-Tx and PS-Rx (SS-BS) | Okumura-Hata model |
| Path-loss between PS-Rx and SS-BS | Free space propagation loss |
| Channel model | Ring model |

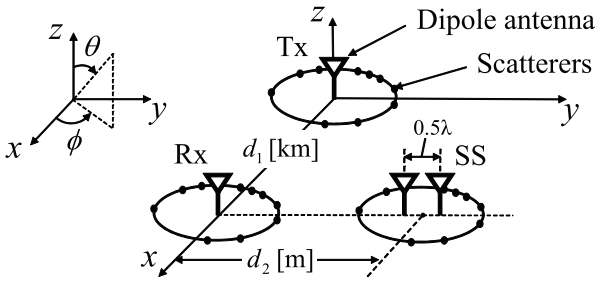


**Fig. 3** Channel model and antenna arrangement.

$\boldsymbol{H}_{ST}$, where the height of PS-Tx is 100 m and that of PS-Rx and SS-BS are 10 m. A free space propagation model is adopted for $\boldsymbol{H}_{SR}$ for simplicity.

Figure 3 shows the channel model and the arrangement of antennas and scatterers. The channels are calculated by a geometry-based ring model [15], [16] and the path-loss is taken into account as described above. After that, the influence of the channel due to load modulation can be calculated by (3). The separation distance of PS-Tx and PS-Rx is denoted by $d_1$ [km] and that of PS-Rx and SS-BS is denoted by $d_2$ [m]. Also, we consider the distance of between PS-Tx and SS-BS is approximately equal to $d_1$. In the ring model, 10 scatterers are distributed on the horizontal plane around each antenna, and ring size is assumed to be sufficiently large compared to antenna size, i.e. all paths can be recognized as plane waves. For each trial, the channel is generated randomly by arranging the scatterers in random directions [17], [18], i.e. 1000 channels with different path distributions are used for the evaluation. The intensity of the received signals at PS-Rx and SS-BS vary depending on the channel strength and noise for each trial since the strength of the channel generated by this model and noise are not unified in this simulation. Nevertheless, the power expectation of the channel is statistically determined corresponding to the path-loss. Also, the noise power expectation is always constant because it does not depend on the channel.

When we consider the practical use, PS-Rx and SS-BS

antennas can be placed at indoor or outdoor. If SS-BS is placed at outdoor, the transmitted signal from SS-BS may interfere many PS-Rxs because some TV set antennas are in line-of-sight. To suppress the interference, SS-BS is required to have many antennas because it must have sufficient degree of freedom to suppress the interference to multiple PS-Rxs. In this case, the other technique, such as beam-tilting, transmission power control at SS-BS, and so on, should be jointly used to mitigate the interference with the realistic number of the antennas. When SS-BS is located in an indoor environment, the building penetration loss needs to be considered. Although the reception power at PS-Rx is lowered by the penetration loss, the loss is about 8 dB in the UHF band [19]–[21]. On the other hand, the penetration loss can be exploited for confining SS-BS signals into the limited area. This means the SS-BS can be aware of the smallest number of the PS-Rxs, which may be the nearest TV set.

## 4. Results

### 4.1 The Estimation Error at SS

In Sect. 2, we indicated the need to estimate $\boldsymbol{H}'_{SR}$ from PS-Tx by way of PS-Rx in order to control interference by BF. However, channel error due to noise is inevitable when receiving signals at SS-BS. The estimation error is expressed as [9], [22],

$$J = \frac{\|\boldsymbol{H}_{error} - \boldsymbol{H}_{true}\|_F^2}{\|\boldsymbol{H}_{true}\|_F^2}, \tag{9}$$

where $\boldsymbol{H}_{error}$ is the channel containing error and $\boldsymbol{H}_{true}$ is the true channel to be estimated, i.e., $\boldsymbol{H}'_{SR}$.

Figure 4 shows the CDF (Cumulative Distribution Function) of the estimation error with various numbers of training sets, $L$. Here, the intersystem distances are $d_1 = 1$ km and $d_2 = 10$ m. Training is the process of estimating the propagation channel at the receiving side (at SS-BS) when PS-Tx transmits a known signal, and $L$ represents the number of transmission symbols that are used for training. In this study, PS-Tx transmits the symbols, $\boldsymbol{X} = [x_1, x_2, \cdots, x_L]$. From Fig. 4, it can be seen that the 50% estimation error at $L = 100$ is a 22.0 dB improvement compared to that at $L = 1$. That is, the estimation error is reduced by increasing $L$, and $L$ is set to 100 in the following discussions.

Figure 5 shows the CDF of the channel estimation error with various intersystem distances. It can be seen that the 50% estimation error is −8.3 dB at $d_1 = 3$ km, $d_2 = 50$ m whereas $J = -38.1$ dB at $d_1 = 1$ km, $d_2 = 10$ m. That is, the estimation error is raised since the path-loss increases with $d_1$ and $d_2$. Thus, the estimation error falls as $d_1$ and $d_2$ are decreased.

### 4.2 SIR at PS-Rx

This section discusses SIR at PS-Rx with and without interference control. Here, the desired signal power and the interference power are calculated by using $\boldsymbol{H}_{RT}$ and $\boldsymbol{H}_{SR}^T$, respectively. The transmitted power of SS-BS is 10 dBm.

Figure 6 shows the relation between the channel estimation error and SIR with interference control. In this figure, it is found that the lower estimation error is, the higher SIR becomes. Here, according to [23], in a televi-

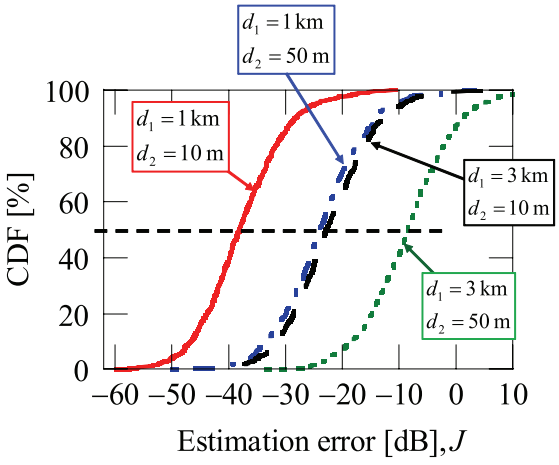


**Fig. 5** CDF of the channel estimation error with various intersystem distances, $d_1$ and $d_2$.

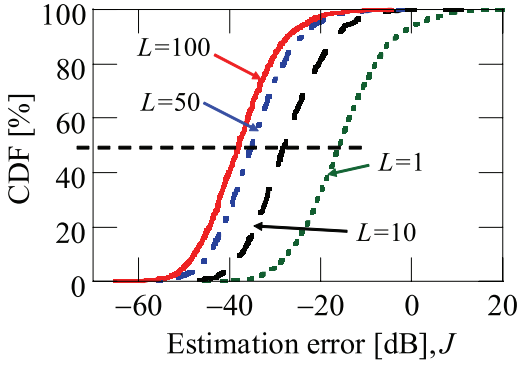


**Fig. 4** CDF of the estimation error with various numbers of training sets, $L$.

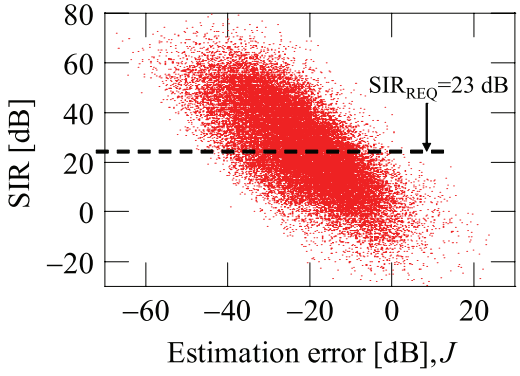


**Fig. 6** The relation between the channel estimation error and SIR with interference control.

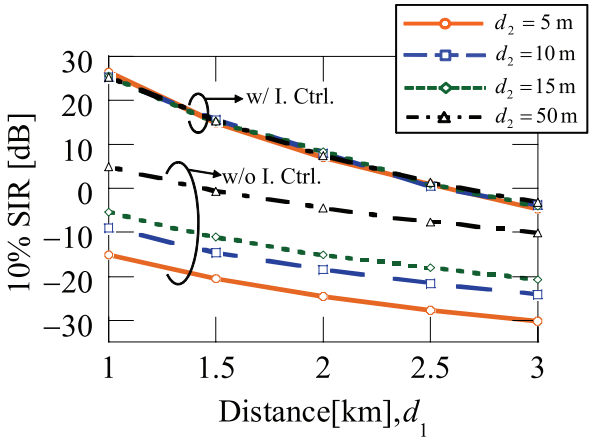


**Fig. 7** 10% SIR at PS-Rx versus $d_1$.

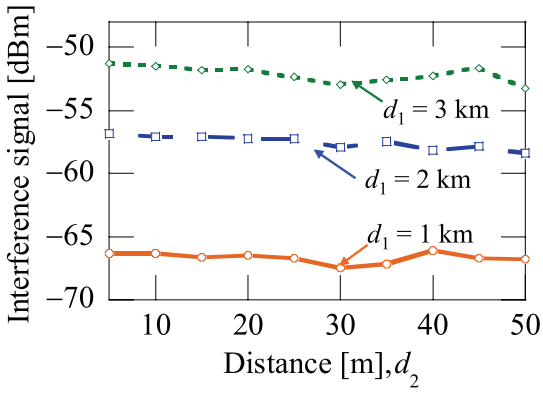


**Fig. 8** Interference signal at PS-Rx with interference control versus $d_2$.

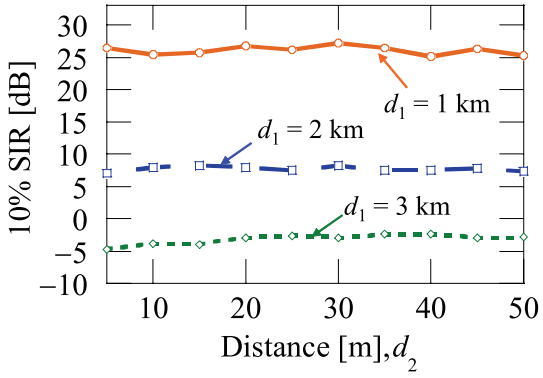


**Fig. 9** 10% SIR at PS-Rx with interference control versus $d_2$.

sion broadcast system, the required SIR, which is defined as $\mathrm{SIR}_{\mathrm{REQ}}$, must be above 23 dB at PS-Rx. In order to reveal the applicable range of proposed method, the required estimation error, $J_{REQ}$ is calculated by median value when $\mathrm{SIR}_{\mathrm{REQ}} = 23$ dB. From Figs. 5 and 6, it can be seen that $J_{REQ} = -19.5$ dB, and the applicable range of proposed method is determined as: $d_1 = 3$ km or less when $d_2 = 10$ m. Or $d_2 = 50$ m or less when $d_1 = 1$ km.

Next, the distance characteristics of SIR are discussed in the view of the applicable ranges. Figure 7 shows the SIR at PS-Rx versus $d_1$. Also, SIR in following discussion is evaluated using the 10% value in CDF because we need to confirm that the effect of interference reduction by proposed method is sufficient even if the interference from SS-BS is in a worst case such as LOS environment. It is found that SIR with interference control is independent of $d_2$ from Fig. 7. The reason is as follows:

(1) The path-loss becomes small (large) as $d_2$ becomes closer (more distant).

(2) The interference to PS-Rx becomes large (small), but the component of $\boldsymbol{H}'_{SR}$ which is necessary for interference suppression, also becomes large (small).

(3) Figure 8 shows the interference signal at PS-Rx with interference control versus $d_2$. It is found that the interference signal with interference control is independent of $d_2$ since the interference to PS-Rx and the level of interference suppression by proposed method cancel each other.

(4) Figure 9 shows 10% SIR at PS-Rx with interference control versus $d_2$. SIR can be calculated from the ratio of the desired signal and the interference signal. From Fig. 8, it was found that the interference to PS-Rx with interference control is independent of $d_2$, and the desired signal is naturally no change for $d_2$. Therefore, it can also be seen that SIR with interference control becomes independent of $d_2$.

In addition, the reason that the SIR at PS-Rx is independent of $d_2$ can be understood in detail by the following discussion. The interference signal with interference control from SS-BS to PS-Rx can be expressed as,

$$\boldsymbol{y}_{i_{RS}} = \boldsymbol{H}_{SR}^{T}\tilde{\boldsymbol{V}}_{RS}\boldsymbol{s}_S = -\frac{\sqrt{2}\boldsymbol{n}^T\tilde{\boldsymbol{V}}_{RS}\boldsymbol{s}_S}{(1-S_{RR})^{-1}\sqrt{P_T A_{RT}}}, \tag{10}$$

where $\tilde{\boldsymbol{V}}_{RS}$ and $\boldsymbol{s}_S$ represent the null-space weight vectors, which is obtained from (8) and transmitted signal at SS-BS, respectively. $\boldsymbol{n}$ is the noise at SS-BS. $A_{RT}$ denotes path-loss between PS-Tx and PS-Rx, i.e. $A_{RT} = (P_R$: received power at PS-Rx)/($P_T$: transmitted power at PS-Tx). The derivation of (10) is described in appendix. From (10), it is clarified that the interference signal from SS-BS to PS-Rx is independent of the path-loss between PS-Rx and SS-BS, i.e. $d_2$ does not affect SIR.

Furthermore, in Fig. 7, it can be seen that the effect of interference reduction by proposed method is remarkable when both $d_1$ and $d_2$ are sufficiently short, e.g., SIR with interference control is 26.5 dB, which is 41.5 dB higher than that without interference control at $d_1 = 1$ km and $d_2 = 5$ m. Therefore, the proposed method is effective in controlling interference between PS-Rx and SS-BS when intersystem distances are short.

### 4.3 Transmission Characteristics at SS

This section focuses on the transmission characteristics at SS when the base station of SS controls transmitted power so as to achieve the desired SIR at PS-Rx. Figure 10 shows a transmission system model at SS. SS-BS is the base sta-

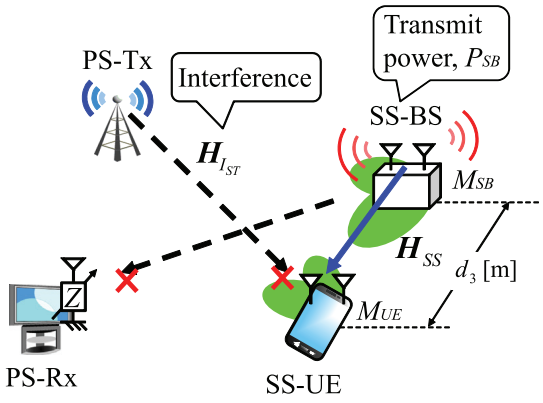


**Fig. 10** Transmission system model at SS.

tion, SS-UE is the user equipment, and both systems have two antennas each ($M_{SB} = M_{UE} = 2$). The operation frequency of SS is 700 MHz. The propagation channel $\boldsymbol{H}_{I_{ST}}$ is the interference channel from PS-Tx to SS-UE. In this paper, the channel estimation error of $\boldsymbol{H}_{I_{ST}}$ is inevitable due to the noise. Nevertheless, SS-UE can estimate ideal $\boldsymbol{H}_{I_{ST}}$ by training for a long time. This will enable SS-UE to suppress $\boldsymbol{H}_{I_{ST}}$, and the interference suppression process at SS-UE is described in the following. By the SVD of $\boldsymbol{H}_{I_{ST}}$, we get,

$$\boldsymbol{H}_{I_{ST}} = [\bar{\boldsymbol{U}}_{I_{ST}}, \tilde{\boldsymbol{U}}_{I_{ST}}][\boldsymbol{S}_{I_{ST}}, 0]^T \boldsymbol{V}_{I_{ST}}^H, \tag{11}$$

where $\tilde{\boldsymbol{U}}_{I_{ST}}$ is the null-space weight vectors from PS-Tx. The equivalent channel between PS-Tx and SS-UE becomes,

$$\boldsymbol{H}'_{I_{ST}} = \tilde{\boldsymbol{U}}_{I_{ST}}^H \boldsymbol{H}_{I_{ST}}, \tag{12}$$

when the receiver weight, $\tilde{\boldsymbol{U}}_{I_{ST}}$, is used. In this study, we assume the ideal environment, i.e., SS-UE completely cancels the interference, $\boldsymbol{H}_{I_{ST}}$. Also, $\boldsymbol{H}_{SS}$ represents the self-link channel at SS, and the equivalent is expressed as,

$$\boldsymbol{H}'_{SS} = \tilde{\boldsymbol{U}}_{I_{ST}}^H \boldsymbol{H}_{SS} \tilde{\boldsymbol{V}}_{RS}. \tag{13}$$

$\boldsymbol{H}_{I_{ST}}$ and $\boldsymbol{H}_{SS}$ are also calculated by the ring model and the path-loss is taken into account. By using (13), the channel capacity at SS can be approximately calculated by [24],

$$C = \log_2 \left| \boldsymbol{H}'_{SS} \boldsymbol{H}'^H_{SS} \frac{P_{SB}}{(M_{SB} - N_{Null})\sigma_n^2} + \boldsymbol{I}_{SS} \right|, \tag{14}$$

where $P_{SB}$ is the transmitted power of SS-BS and $N_{null}$ is the degree of freedom which SS-BS uses in order to suppress the interference. $\boldsymbol{I}_{SS}$ is an identity matrix and $\sigma_n^2$ is the power of Gaussian noise.

Figure 11 shows average SNR at SS versus the distance between SS-BS and SS-UE, $d_3$. In this figure, the solid and dashed lines represent the SNR with PS and proposed scheme and the without PS, where the transmitting power of SS-BS, $P_{SB}$ is given identically for both scenarios. Here, the SNR with PS is calculated by assuming SS-BS suppresses interference against PS-Rx and SS-UE cancels the interference from PS-Tx, i.e. SS-BS and SS-UE have only one remaining degree of freedom for their communication link.

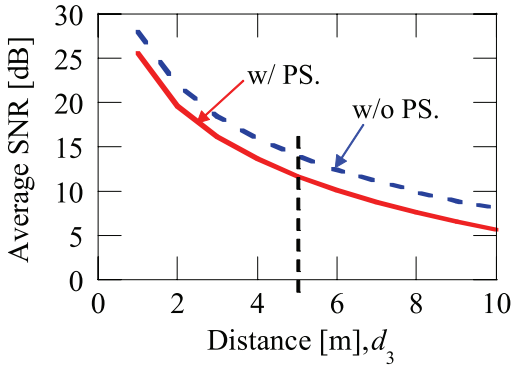


**Fig. 11** Average SNR at SS versus $d_3$.

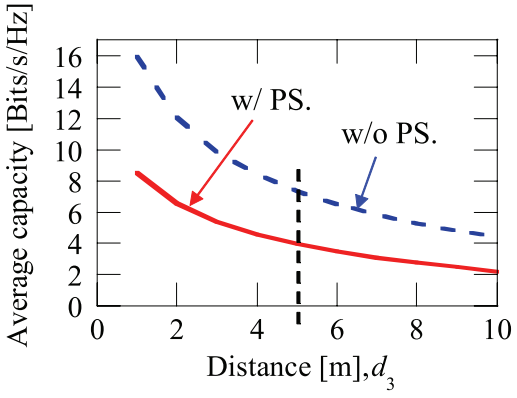


**Fig. 12** Average channel capacity at SS versus $d_3$.

On the other hand, the SNR without PS in calculated by assuming SS-BS and SS-UE do not suppress the interference because they have neither the PS-Rx nor PS-Tx, i.e. both of the SS-BS and SS-UE can use the full degree of freedom for their communication link. Therefore, the communication links of SS with PS and without PS are SISO (Single-Input Single-Output) and MIMO (Multiple-Input Multiple-Output), respectively. The intersystem distances are set to $d_1 = 1$ km and $d_2 = 5$ m, and $P_{SB} = 10$ dBm. When we focus on the solid lines at $d_3 = 5$ m, it can be seen that the SNR values are 11.7 and 14.0 dB at SS-BS with PS and without PS, respectively. Note that no interference control is performed for the scenario without PS. It is found that the SNR without PS is a little higher than that with PS since there is no decrease in degree of freedom of SS-BS antennas by nulling.

Figure 12 shows average capacity at SS versus $d_3$. In this figure, the solid and dashed lines represent the capacity with and without PS, respectively. The simulation conditions are given identically to Fig. 11. When we focus on the solid lines at $d_3 = 5$ m, it can be seen that the capacities with and without PS are 4.0 and 7.3 bits/s/Hz in SS, respectively. The reason that capacity with PS is 3.3 bits/s/Hz lower than that without PS is in common with consideration of Fig. 11. It is also found that the capacity is decreased due to the existence of PS, however, it is possible to ensure the enough capacity in all distances. These results indicate that the pro-

pose method allows SS to suppress the interference to PS-Rx and communicate sufficiently.

## 5. Conclusion

In this paper, the interference control method using load modulation has been presented for coexistence of PS-Rx with SS-BS. In this method, a load modulation technique is used to let us establish the interference channel between PS-Rx and SS-BS. Also, SS-BS estimates the interference channel by observing the modulated signals at PS-Rx side, and uses null-space vector as transmitting weights that are obtained from the channel. A simulation of SIR with interference control showed a significant SIR improvement regardless of $d_2$. In particular, the interference reduction offered by the proposed method is remarkable if the intersystem distances are short, e.g., SIR with interference control is 26.5 dB, and this SIR is 41.5 dB higher than that without interference control at $d_1 = 1$ km and $d_2 = 5$ m. Thus, it is possible to reduce the interference to PS-Rx by using proposed method. Furthermore, this paper has evaluated average channel capacity at SS. It is found that the average capacity with interference is reduced due to the degrees of freedom of SS-BS antennas control compared to absence of PS-Tx and PS-Rx (without interference control). However, it can also be seen that capacity with interference control is 4.0 bits/s/Hz when $d_3 = 5$ m. Therefore, in nulling to PS-Rx, it is possible to obtain the data rate at the SS if it is a short-range environment.

These results show that the interference control using proposed method is effective especially in close-range configurations, and is suited to small cells that share a frequency.

## Acknowledgements

This research was partially supported by JSPS KAKENHI (25709030).

### References

[1] K. Nishimori, H. Yomo, P. Popovski, Y. Takatori, R. Prasad, and S. Kubota, "Interference cancellation and avoidance for secondary users co-existing with TDD-based primary systems," Wireless Pers. Commun., vol.45, no.3, pp.403–421, May 2008.
[2] J. Mitola, III, "Cognitive radio for flexible mobile multimedia communications," Proc. IEEE International Workshop on Mobile Multimedia Communications (MoMuC), pp.3–10, Nov. 1999.
[3] S. Haykin, "Cognitive radio: brain-empowered wireless communications," IEEE J. Sel. Areas Commun., vol.23, no.2, pp.201–220, Feb. 2005.
[4] Y. Beyene, K. Ruttik, and R. Jantti, "Effect of secondary transmission on primary pilot carriers in overlay cognitive radios," 2013 8th International Conference, Cognitive Radio Oriented Wireless Networks (CROWNCOM), pp.111–116, July 2013.
[5] K. Terasaki and N. Honma, "Feasible load modulation technique using multiple antenna systems," IET J. Electronics Letters, vol.48, no.18, pp.1090–1091, Aug. 2012.
[6] T. Ito, N. Honma, K. Terasaki, K. Nishimori, and Y. Tsunekawa, "Use of load modulation for interference control between primary and secondary systems," 2013 Asia-Pacific Microwave Conference (APMC 2013), Electric Proc. APMC 2013, F2F-3, Nov. 2013.
[7] G.R. Simpson, "A generalized n-port cascade connection," IEEE MTT-S Int. Microwave Symp. Dig., pp.507–509, 1981.
[8] J.W. Wallace and M.A. Jensen, "Mutual coupling in MIMO wireless systems: A rigorous network theory analysis," IEEE Trans. Wireless Commun., vol.3, no.4, pp.1317–1325, July 2004.
[9] N. Honma, K. Nishimori, R. Kudo, Y. Takatori, and M. Mizoguchi, "Fast control method of parasitic antennas using noniterative algorithm in multiantenna system," IEEE Trans. Antennas Propag., vol.60, no.4, pp.2044–2051, April 2012.
[10] W. Yamada, K. Nishimori, Y. Takatori, and Y. Asai, "Statistical analysis and characterization of Doppler spectrum in large office environment," Proc. International Symposium on Antennas and Propagation (ISAP'09), pp.564–567, Bangkok, Thailand, 2009.
[11] J.R. James, G.D. Evans, and A. Fray, "Beam scanning microstrip arrays using diodes," Proc. Inst. Elect. Eng. Microwaves, Antennas, Propagat., vol.140, pp.43–51, Feb. 1993.
[12] T. Takeuchi, H. Hamazumi, and K. Shibuya, "Performance improvement of post-FFT adaptive array with reciprocal interpolation for ISDB-T," IEICE Trans. Commun., vol.E95-B, no.11, pp.3527–3535, Nov. 2012.
[13] S. Umeda, S. Suyama, H. Suzuki, and K. Fukawa, "PAPR reduction method for block diagonalization in multiuser MIMO-OFDM systems," Proc. IEEE 71st Vehicular Technology Conference (VTC 2010-Spring), pp.1–5, 2010.
[14] J.-H.C. Zhan and S.S. Taylor, "A 5 GHz resistive-feedback CMOS LNA for low-cost multi-standard applications," IEEE ISSCC 2006 Dig. Tech. Papers, pp.200–201, Feb. 2006.
[15] P. Dent, G.E. Bottomley, and T. Croft, "Jakes fading model revisited," Electron. Lett., vol.29, no.13, June 1993.
[16] A.F. Molisch, "A generic model for MIMO wireless propagation channels in macro- and microcells," IEEE Trans. Signal Process., vol.52, no.1, pp.61–71, Jan. 2004.
[17] M. Patzold and B.O. Hogstad, "A space-time channel simulator for MIMO channels based on the geometrical one-ring scattering model," Wireless Communications and Mobile Computing, Special Issue on Multiple-Input Multiple-Output (MIMO) Communications, vol.4, no.7, pp.727–737, Nov. 2004.
[18] M. Patzold and B.O. Hogstad, "A wideband MIMO channel model derived from the geometric elliptical scattering model," Proc. IEEE ISWCS'06, pp.138–143, Valencia, Spain, Sept. 2006.
[19] Y. Zhang and Y. Hwang, "Measurements of the characteristics of indoor penetration loss," 1994 IEEE 44th, Vehicular Technology Conference, vol.3, pp.1741–1744, Stockholm, Sweden, June 1994.
[20] J. Horikoshi, K. Tanaka, and T. Morinaga, "1.2 GHz band wave propagation measurements in concrete building for indoor radio communications," IEEE Trans. Veh. Technol., vol.VT-35, pp.146–152, Nov. 1986.
[21] D. Plets, W. Joseph, L. Verloock, L. Martens, H. Gauderis, and E. Deventer, "Extensive penetration loss measurements and models for different building types for DVB-H in the UHF band," IEEE Trans. Broadcast., vol.55, no.2, pp.213–222, June 2009.
[22] N. Honma, "Method of MIMO channel estimation between parasitic antenna arrays," IEEE Trans. Antennas Propag., vol.61, no.5, pp.2792–2800, May 2013.
[23] S. Shellhammer, S. Shankar, R. Tandra, and J. Tomcik, "Performance of power detector sensors of DTV signals in IEEE 802.22 WRANs," Proc. First ACM International Workshop on Technology and Policy for Accessing Spectrum (TAPAS), Aug. 2006.
[24] N. Honma, T. Murakami, M. Mizoguchi, and Y. Tsunekawa, "Effect of antenna spacing on inter-cell interference in wireless LAN using transmitting beam forming," 2011 International Symposium on Antennas and Propagation (ISAP 2011), Electric Proc. ISAP 2011, WeE2-5, Oct. 2011.

## Appendix: The Derivation of (10)

This appendix shows the derivation of (10). From (5) in this paper, the observed propagation channel at SS-BS is expressed as,

$$\boldsymbol{H}'_{ST} = \boldsymbol{H}_{ST} + \boldsymbol{H}_{SR}(1 - S_{RR})^{-1}H_{RT}, \tag{A·1}$$

where the state of load impedance, $Z$ at PS-Rx is switched to open. This channel is added to noise, so the received signal at SS-BS is expressed as,

$$\boldsymbol{y}_{SB} = \{\boldsymbol{H}_{ST} + \boldsymbol{H}_{SR}(1 - S_{RR})^{-1}H_{RT}\}s_T + \boldsymbol{n}, \tag{A·2}$$

where $s_T$ is the transmitted signal of PS-Tx, and its power represents $P_T$. $\boldsymbol{n}$ is the noise per SS-BS antenna and has dispersion, $\sigma_n^2$. It is expressed as,

$$\boldsymbol{n} = [n_1, n_2, \cdots, n_{M_{SB}}]^T, \tag{A·3}$$

where $n_i$ $(i = 1, 2, \cdots, M_{SB})$ is in a Gaussian distribution and $M_{SB}$ denotes the number of SS-BS. Here, it is possible to consider $s_T$ as known signal when SS-BS can decode the $s_T$. For sake of simplicity, we define $s_T$ as $\sqrt{P_T}$, and (A·2) is transformed into,

$$\boldsymbol{H}'_{ST} = \boldsymbol{H}_{ST} + \boldsymbol{H}_{SR}(1 - S_{RR})^{-1}\sqrt{A_{RT}} + \frac{\boldsymbol{n}}{\sqrt{P_T}}, \tag{A·4}$$

where $A_{RT}$ is path-loss between PS-Tx and PS-Rx, i.e. $A_{RT}$ = ($P_R$: received power at PS-Rx)/($P_T$: transmitted power at PS-Tx), and $H_{RT} = \sqrt{A_{RT}}$. As shown by (6), the term $\boldsymbol{H}_{ST}$ can be eliminated from (A·4) since $\boldsymbol{H}_{ST}$ is directly observed by switching the termination to load (50 Ω) state at PS-Rx. Therefore, $\boldsymbol{H}'_{SR}$ estimated by SS-BS is expressed as,

$$\boldsymbol{H}'_{SR} = \boldsymbol{H}_{SR}(1 - S_{RR})^{-1}\sqrt{A_{RT}} + \frac{\boldsymbol{n}'}{\sqrt{P_T}}, \tag{A·5}$$

where $\boldsymbol{n}'$ is expressed as,

$$\boldsymbol{n}' = \boldsymbol{n}_{open} - \boldsymbol{n}_{load} \tag{A·6}$$

since (A·5) is obtained by subtracting two different channels (i.e. $\boldsymbol{H}'_{ST(open)}$ and $\boldsymbol{H}'_{ST(load)}$) that contain different noises. Also, the power expectation of (A·6) is calculated by,

$$\begin{aligned} &E\left[|\boldsymbol{n}_{open} - \boldsymbol{n}_{load}|^2\right] \\ &= E\left[|\boldsymbol{n}_{open}|^2 - \boldsymbol{n}_{open}\boldsymbol{n}^*_{load} - \boldsymbol{n}_{load}\boldsymbol{n}^*_{open} + |\boldsymbol{n}_{load}|^2\right] \\ &= E\left[|\boldsymbol{n}_{open}|^2 + |\boldsymbol{n}_{load}|^2\right] \\ &= 2\sigma_n^2, \end{aligned} \tag{A·7}$$

then, $\boldsymbol{n}'$ can be expressed as,

$$\boldsymbol{n}' = \sqrt{2}\boldsymbol{n}. \tag{A·8}$$

The interference from SS-BS to PS-Rx is discussed in this following. In this study, the transposed matrix of $\boldsymbol{H}_{SR}$, $\boldsymbol{H}^T_{SR}$ represents the interference channel. By (A·5) and (A·8), $\boldsymbol{H}^T_{SR}$ is expressed as,

$$\boldsymbol{H}^T_{SR} = \frac{\boldsymbol{H}'^T_{SR}}{(1-S_{RR})^{-1}\sqrt{A_{RT}}} - \frac{\sqrt{2}\boldsymbol{n}^T}{(1-S_{RR})^{-1}\sqrt{P_T A_{RT}}}. \tag{A·9}$$

Furthermore, from (8) in this paper, SS-BS can suppress interference by using $\tilde{\boldsymbol{V}}_{RS}$ as the transmitting weight, which represents null-space eigenvector and is calculated from singular-value-decomposition of $\boldsymbol{H}'^T_{SR}$. The interference signal is calculated by,

$$\begin{aligned} \boldsymbol{y}_{i_{RS}} &= \boldsymbol{H}^T_{SR}\tilde{\boldsymbol{V}}_{RS}\boldsymbol{s}_S \\ &= \frac{\boldsymbol{H}'^T_{SR}\tilde{\boldsymbol{V}}_{RS}\boldsymbol{s}_S}{(1-S_{RR})^{-1}\sqrt{A_{RT}}} - \frac{\sqrt{2}\boldsymbol{n}^T\tilde{\boldsymbol{V}}_{RS}\boldsymbol{s}_S}{(1-S_{RR})^{-1}\sqrt{P_T A_{RT}}} \qquad (A·10) \\ &= -\frac{\sqrt{2}\boldsymbol{n}^T\tilde{\boldsymbol{V}}_{RS}\boldsymbol{s}_S}{(1-S_{RR})^{-1}\sqrt{P_T A_{RT}}}. \qquad (A·11) \end{aligned}$$

$\boldsymbol{s}_S$ is the transmitted signal of SS-BS, and defined as,

$$\boldsymbol{s}_S = [s_{S,1}, s_{S,2}, \cdots, s_{S,M_{SB}}]^T, \tag{A·12}$$

where $s_{S,i}$ $(i = 1, 2, \cdots, M_{SB})$ is in a Gaussian distribution. From (A·10) and (A·11), the term $\frac{\boldsymbol{H}'^T_{SR}\tilde{\boldsymbol{V}}_{RS}\boldsymbol{s}_S}{(1-S_{RR})^{-1}\sqrt{A_{RT}}}$ is eliminated due to orthogonality between $\boldsymbol{H}'^T_{SR}$ and $\tilde{\boldsymbol{V}}_{RS}$. As a result, (10) in this paper is derived.

**Takuma Ito** received the B.E. in electrical and electronic engineering from Iwate University, Morioka, Japan in 2013. He is currently in the master program in Iwate University. His research interest is interference control using load modulation.

**Naoki Honma** received the B.E., M.E., and Ph.D. degrees in electrical engineering from Tohoku University, Sendai, Japan in 1996, 1998, and 2005, respectively. In 1998, he joined the NTT Radio Communication Systems Laboratories, Nippon Telegraph and Telephone Corporation (NTT), in Japan. He is now working for Iwate University. He received the Young Engineers Award from the IEICE of Japan in 2003, the APMC Best Paper Award in 2003, and the Best Paper Award of IEICE Communication Society in 2006, respectively. His current research interest is planar antennas for high-speed wireless communication systems. He is a member of IEEE.

**Keisuke Terasaki** received the B.E. in electrical and electronic engineering from Iwate University, Morioka, Japan in 2012. He is currently in the master program in Iwate University. His research interest is feasible load modulation techniques for multiple antenna systems.

**Kentaro Nishimori** received the B.E., M.E. and Ph.D. degrees in electrical and computer engineering from Nagoya Institute of Technology, Nagoya, Japan in 1994, 1996 and 2003, respectively. In 1996, he joined the NTT Wireless Systems Laboratories, Nippon Telegraph and Telephone Corporation (NTT), in japan. He was senior research engineer on NTT Network Innovation Laboratories. He is now associate professor in Niigata University. He was a visiting researcher at the Center for Teleinfrastructure (CTIF), Aalborg University, Aalborg, Denmark from Feb. 2006 to Jan. 2007. He was an Associate Editor for the Transactions on Communications for the IEICE Communications Society from May 2007 to May 2010 and Assistant Secretary of Technical Committee on Antennas and Propagation of IEICE from June 2008 to May 2010. He received the Young Engineer Award from IEEE AP-S Japan Chapter in 2001, Best Paper Award of Software Radio Society in 2007 and Distinguished Service Award from the IEICE Communications Society in 2005, 2008 and 2010. His main interests are spatial signal processing including MIMO systems and interference management techniques in heterogeneous networks. He is a member of IEEE. He received IEICE Best Paper Award in 2010.

**Yoshitaka Tsunekawa** received the B.E. degree from Iwate University, Morioka, Japan, in 1980 and the M.E. and the Doctor of Engineering degrees from Tohoku University, Sendai, Japan, in 1983 and 1993, respectively. Since 1983, he has been with the Faculty of Engineering, Iwate University, where he is now a professor at the Department of Electrical Engineering and Computer Science. His current research interests include digital signal processing and digital control. He is a member of the Institute of Electronics, Information and Communication Engineers of Japan, and IEEE.